Purified Thick Filaments from the Nematode *Caenorhabditis elegans*: Evidence for Multiple Proteins Associated with Core Structures

Henry F. Epstein, Gary C. Berliner, Douglas L. Casey, and Irving Ortiz

Department of Neurology, Baylor College of Medicine, Houston, Texas 77030

Abstract. The thick filaments of the nematode, *Caenorhabditis elegans*, arising predominantly from the body-wall muscles, contain two myosin isoforms and paramyosin as their major proteins. The two myosins are located in distinct regions of the surfaces, while paramyosin is located within the backbones of the filaments. Tubular structures constitute the cores of the polar regions, and electron-dense material is present in the cores of the central regions (Epstein, H. F., D. M. Miller, I. Ortiz, and G. C. Berliner. 1985. *J. Cell Biol.* 100:904–915). Biochemical, genetic, and immunological experiments indicate that the two myosins and paramyosin are not necessary core components (Epstein, H. F., I. Ortiz, and L. A. Traeger Mackinnon. 1986. *J. Cell Biol.* 103:985–993). The existence of the core structures suggests, therefore, that additional proteins may be associated with thick filaments in *C. elegans*.

To biochemically detect minor associated proteins, a new procedure for the isolation of thick filaments of high purity and structural preservation has been developed. The final step, glycerol gradient centrifugation, yielded fractions that are contaminated by, at most, 1–2% with actin, tropomyosin, or ribosome-associated proteins on the basis of Coomassie Blue staining and electron microscopy. Silver staining and radioautography of gel electrophoretograms of unlabeled and ^{35}S-labeled proteins, respectively, revealed at least 10 additional bands that cosedimented with thick filaments in glycerol gradients. Core structures prepared from wild-type thick filaments contained at least six of these thick filament-associated protein bands. The six proteins also cosedimented with thick filaments purified by gradient centrifugation from CB190 mutants lacking myosin heavy chain B and from CB1214 mutants lacking paramyosin. For these reasons, we propose that the six associated proteins are potential candidates for putative components of core structures in the thick filaments of body-wall muscles of *C. elegans*.

MYOSIN-CONTAINING filaments have been a major focus of research for over 30 years (11). The demonstration that myosin was contained in one set of filaments was critical to the foundation of the sliding-filament theory of muscle contraction (15). The isolation of natural filaments containing myosin and the formation of synthetic filaments from purified myosin were key confirmations of the theory and raised the important question as to whether the intrinsic self-assembly of myosin molecules explained the formation of thick filaments in vivo (14).

The discovery that additional, nonmyosin proteins are components of natural thick filaments in both vertebrate and invertebrate muscles suggests that the assembly of these filaments may be more complex than simple self-assembly of myosin. For example, recent studies of rabbit skeletal muscles indicate that epitopes of the C, H, and X proteins are localized at very specific and distinct positions near the surface of specific thick filaments (1). Studies of various invertebrate muscles show that paramyosin is a major protein component of the backbones of the thick filaments (30). In other invertebrate muscles, paramyosin may be present only as a relatively minor protein (3, 12, 25). The diversity of nonmyosin protein components of thick filaments, their locations, and their relative amounts supports the alternative hypothesis that the assembly of thick filaments, in general, may require a sequence of specific reactions involving both myosin and other proteins. Assembly of thick filaments in a particular muscle may be a specialized process requiring a particular combination of proteins and the specific structural interactions between them.

The thick filaments of the body-wall muscles of the nematode *Caenorhabditis elegans* exhibit several characteristics that suggest a sequence of reactions involving specific proteins in a specialized assembly process. Two myosins containing different isoforms of myosin heavy chain are located in distinct regions of the thick filaments (21). Paramyosin is located within the backbones of the filaments (18). A tubular structure that is morphologically distinct from the predominant myosin and paramyosin substructures constitutes the core of the polar regions of the thick filaments (Fig. 1).

Electron-dense material appears within the tubular core structures in the central regions of the filaments (4). Biochemical, genetic, and immunological experiments show that the structures of the polar and central cores do not require myosin heavy chain B or paramyosin (4, 5). A proposed relationship between the substructures of nematode thick filaments is depicted schematically in Fig. 1.

The existence of core structures separate from myosin and paramyosin is part of a general model for the structure of all thick filaments (29). The possibility of a core template in myosin assembly was originally hypothesized from studies describing synthetic filament formation with rabbit skeletal muscle myosin (16). Indeed, the search for possible proteins of such a core was attempted years ago in rabbit psoas muscle (23). We report here on an improved isolation and purification of thick filaments from *C. elegans* that was necessary for the resulting identification of several nonmyosin proteins as potential candidates for putative core components. We have used glycerol gradient sedimentation (23) to separate thick filaments from thin filaments, ribosomes, and chromatin. The prior elimination of proteolytic activity, removal of intact nuclei, and enrichment of fractions for thick filaments in high concentration were all necessary for the ultimate isolation. 10 protein bands were detected by either (*a*) Coomassie Blue and silver staining of unlabeled material or (*b*) radioautography of ^{35}S-labeled material that had been subjected to electrophoresis. These 10 protein bands were enriched in gradient fractions that by electron microscopy contained the most thick filaments and by gel electrophoresis contained the highest concentrations of myosin heavy and light chains and paramyosin. These additional bands do not react with specific antimyosin antibodies, and at least six of the bands are present in mutants lacking either myosin B (the major body-wall form) or paramyosin. KSCN dissociation of the thick filaments produced structures retaining 30-nm-diam central regions with 14-nm-diam polar core structures. Gel electrophoresis of dissociated filaments showed that substantial fractions of myosin, paramyosin, and other proteins were solubilized, but at least six thick filament-associated proteins sedimented with the core structures and were not solubilized.

Materials and Methods

Nematode Growth and Strains

Wild-type N2 strain of *C. elegans* (2), CB190 (*el90, unc-54* I) myosin B-deficient mutant strain (28), and CB1214 (*el214, unc-15* I) paramyosin-deficient strain (36) were used. Nematodes were grown on eightfold peptone-enriched nematode growth medium (27). Best results were obtained with young adult nematodes; semisynchronized cultures were developed by seeding the plates with dauer larvae and collecting when most nematodes were just past the L4 molt by inspection under a dissecting microscope. The nematodes were collected and frozen as described previously (5). For ^{35}S labeling, N2 nematodes were grown on media deficient in peptone and sulfate with *Escherichia coli* labeled to 625 mCi/mmol (8).

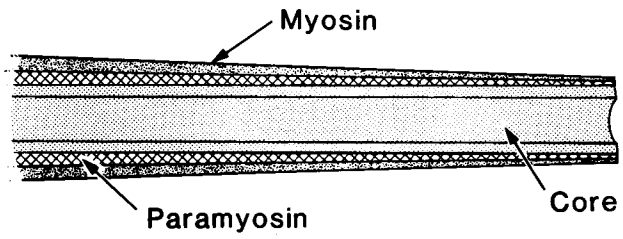

Figure 1. Model of structural domains in nematode thick filaments. Schematic diagram of polar regions of thick filament showing outer myosin, intermediate paramyosin, and innermost core domains. Actual interactions between the different types of proteins comprising the backbone may be more complex. (Figure reprinted from reference 4.)

Thick Filament Isolation

All procedures were performed at 0°C (in ice water mixture), at 4°C (on ice or instrument reading), or as indicated. The pH values of all solutions were determined at 25°C and then the solutions were cooled. All solutions used glass-distilled water. Frozen nematodes were sectioned as described previously (5). 1 g of sectioned nematodes was suspended in 10 ml of relaxing buffer (100 mM KCl, 10 mM $MgCl_2$, 1 mM Na_2EDTA, 6.7 mM potassium phosphate, 1 mM dithiothrietol [DTT], 1 mM phenylmethylsulfonyl fluoride [PMSF], 5 mM ATP, 1 μg/ml soybean trypsin inhibitor, 1 μg/ml leupeptin, 1 μg/ml chymostatin, 1 μg/ml pepstatin, 1 μg/ml *N*-benzoyl-L-arginine ethyl ester, 1 μg/ml *p*-toluidinyl sulfonyl-L-arginine methyl ester (Sigma Chemical Co., St. Louis, MO), pH 6.34, 0°C. The sections were washed twice by sedimentation in 50-ml conical centrifuge tubes (Corning Glass Works, Corning, NY) in a centrifuge (International Equipment Co., Needham Heights, MA) at setting No. 4 for 4 min. The resulting pellet was resuspended in 10 ml of relaxing buffer and 1 ml of 10% (vol/vol) Triton X-100 (7). The suspension was incubated at 0°C for 30 min with gentle mixing by inversion at 10-min intervals. The sections were collected again as above, the procedure was repeated, and the resulting treated sections were resuspended in 3.0 ml of relaxing buffer, 0.5 M sucrose and 0.5% (vol/vol) Triton X-100, and incubated for 10 min at 0°C. The suspension was then homogenized in a 7-ml glass chamber (Dounce, Vineland, NJ) with a glass A pestle (Wheaton Instruments, Millville, NJ) by three sets of five strokes each with an interval of 30 s between each set. The homogenate contained most of the sections, some filaments, nuclei, and ribosomes. The homogenization was then repeated. The remaining sections were removed by centrifugation at each homogenization. The second homogenate contained at least twice the number of thick filaments as the first homogenate. Thick filaments may be purified from either homogenate, but the most pure filaments were isolated from the second. All data presented in this report describe thick filaments prepared from second homogenates.

Such solutions were centrifuged at 5,000 *g* for 10 min in the SS 34 rotor of a Sorvall refrigerated centrifuge (model RC-5B; Sorvall Instruments Div., Newtown, CT) at 4°C. The pellet contained at least 95% of the nuclei. The resulting supernatant was centrifuged at 15,000 *g* for 30 min in the SS 34 rotor. The pellet was markedly enriched for thick filaments, and the supernatant contained most of the thin filaments and ribosomes. The pellet was suspended in 0.3 ml of relaxing buffer. All solutions and pellets were held at 0°C between steps.

Glycerol Gradient Sedimentation

Glycerol gradients were constructed by mixing 10 and 30% (vol/vol) glycerol-relaxing buffer solutions, 2.43 ml each. The 30% solution was mixed into the 10% solution and the resulting mixture was pumped inversely at a flow rate of 5 ml/min into a 5.2-ml polycarbonate tube (SmithKline Diagnostics Inc., Sunnyvale, CA). The resuspended 15,000-*g* pellet was layered gently on top of the gradient and sedimented at 16,000 rpm in an SW 50.1 rotor, in an ultracentrifuge (model L5; Beckman Instruments, Palo Alto, CA) for 75 min at acceleration rate 1 with no brake. The gradient fractions were collected dropwise from the bottom of the tube punctured by a 20-gauge needle. Usually 12 fractions of 7 drops each (~0.40-ml fractions) were collected. A pellet was removed and suspended in 0.4 ml relaxing buffer. The material in each fraction was pelleted at 16,000 rpm for 300 min in thick-walled polypropylene tubes in the SW 50.1 rotor at acceleration rate 10 with the brake set. The pelleted material could be resuspended in various buffer solutions for electron microscopy or experiments. Alternatively, the pellets could be immediately solubilized in 0.1 ml of gel sample buffer and prepared for SDS-PAGE (see below). This procedure was useful for both wild-type and mutant preparations.

KSCN Dissociation of Thick Filaments

Isolated thick filaments were obtained from gradient fractions (most purified), the pellet of the gradient, or from the 15,000-*g* pellet. The pelleted

filaments were resuspended gently in 50 mM KSCN, 5 mM ATP, 10 mM $MgCl_2$, and 20 mM Tris-HCl (pH 8.0 or 8.2). The resulting solution was incubated at 0°C for 30 min. The dissociated filaments were sedimented in an SW 50.1 rotor at 32,000 rpm for 30 min. The supernatant was removed carefully, and the pellet was resuspended gently to the original volume with relaxing buffer. The filaments were resedimented and resuspended again. Similar results were obtained with KSCN concentrations between 50 and 100 mM and pH values between 7.5 and 8.2.

Electron Microscopy of Thick Filaments

Previously published procedures for negative staining with uranyl acetate and calibration of magnifications from this laboratory were used (5, 6).

Protein Determinations

5 or 10 μl of sample was added to 1.0 ml of 0.2 M boric acid, pH 9.2. Fluorescamine (Sigma Chemical Co.) was dissolved in neat acetonitrile at a concentration of 0.2 mg/ml (wt/vol). 0.4 ml of the fluorescamine solution was added to the sample diluted in boric acid and mixed thoroughly. The solution was excited at 390 nm, and the emitted fluorescence was read at 475 nm in an Aminco-Bowman spectrofluorimeter (American Instrument Co., Silver Spring, MD). A standard curve was established with purified mouse IgG whose concentration was determined spectrophometrically by using an A_{280} nm of 1.46 for a 1.0 mg/ml (wt/vol) solution.

Protein Gel Electrophoresis and Detection

Protein samples were either dissolved or brought to 62.5 mM Tris-HCl, pH 6.8, 1% (wt/vol) SDS, 1% (vol/vol) 2-mercaptoethanol, 10% (wt/wt) glycerol, 0.002% (wt/vol) bromophenol blue. The sample solutions in heat-stable plastic tubes were placed in boiling water for 2 min, sonicated by seven pulses with a "Sonifier" Cell Disrupter 200 (Branson Sonic Power Co., Danbury, CT) at setting 7, and placed in boiling water for 2 min. The samples were stored at −82°C.

SDS-PAGE was performed on 0.75-mm-thick slab gels that were gradients in both acrylamide (7.5–15%, [wt/vol]) and sucrose (0.1–0.5 M). The gel buffers were a discontinuous Tris-based system (4). Electrophoresis was performed in a water-jacketed Protean II chamber (BioRad Laboratories, Richmond CA). The samples were subjected to electrophoresis through the stacking gel at 10 mA for 90–120 min and through the separating gel at 20 mA for 240–300 min.

Protein detection was by Coomassie Blue staining, silver staining, or radioautography of ^{35}S-labeled samples. For Coomassie Blue staining, gels were incubated with 0.1% (wt/vol) dye in 50% (vol/vol) methanol, 10% (vol/vol) acetic acid for 2–18 h. The gels were then decolorized in 50% methanol, 10% acetic acid and then rehydrated in distilled water. For silver staining, gels were fixed in 50% methanol, 10% acetic acid for at least 1 h, rehydrated, and then treated with 10% (vol/vol) glutaraldehyde for 30–60 min. At least three 30-min rinses with water were then done. The gels were then reacted with 0.8% (wt/vol) silver nitrate, 19 mM NaOH, 0.42% (vol/vol) ammonium hydroxide for 20–30 min. After rinsing with water for 5–10 min, the gels were developed in 0.5% (wt/vol) citric acid, 0.018% formaldehyde according to visual judgment. The development was stopped by 50% methanol for 10 min or 50% methanol, 10% acetic acid for 1 min. The gels were stored in water.

Gels containing ^{35}S-labeled proteins were dried onto 3M filter paper (Whatman International Ltd., Maidstone, United Kindgom). DuPont Cronex 4 film was exposed to the gel in a Cronex Cassette. Exposure was for 3–41 d. The film was developed in DuPont Cronex film developer for 5 min (DuPont Co., Wilmington, DE), stopped in Cronex stop bath for 30 s, and fixed in Cronex fixative and film hardener for 2 min. The films were rinsed with Kodak Photoflow (Eastman Kodak Co., Rochester, NY) and air dried.

Densitometry of wet-stained gels and radioautograms was performed on a model 620 videodensitometer (BioRad Laboratories) in the transmission mode. Densitometry of dried stained gels was performed in the reflectance mode. Both methods gave consistent results.

Immunoblotting

Proteins were transferred from SDS-polyacrylamide gel slabs to 0.45-μm pure nitrocellulose membranes (Micron Separations, Honeoye Falls, NY) by electrophoresis at 20 W, 300 mA for 20–22 h in 25 mM Tris, 192 mM glycine, 20% (vol/vol) methanol, within a trans-blot cell chamber (BioRad Laboratories). After transfer, the nitrocellulose replicas were blocked in 3% (wt/vol) BSA, PBS (18 mM KH_2PO_4, 57 mM Na_2HPO_4, 0.425% NaCl, pH 7.4) for at least 2 h to minimize nonspecific reactions of antibodies. The three antibodies used, 5-6 (antimyosin A), 28.2 (antimyosin B), and 5-23 (antiparamyosin), are all monoclonal proteins previously isolated and characterized in this laboratory (20). The replica was incubated in 20 ml of 3.0 μg/ml of each mAb in 10% (vol/vol) rabbit serum, 3% BSA, PBS for 1–2 h. The strips were washed six times for 5 min, each wash in 0.05% (vol/vol) Tween-20, PBS. The strips were reacted with a 1:500 dilution of rabbit anti-mouse IgG-conjugated to peroxidase (Sigma Chemical Co.) in 20 ml of 10% rabbit serum, 3% BSA, PBS for 1–2 h and then washed as above. After a final water rinse the blots were developed with 3% (wt/vol) 4-chloro-1-napthol, 50 mM Tris-HCl (pH 6.8), 20% methanol, 0.06% (wt/vol) H_2O_2. The reaction proceeded until sufficient intensity was reached and was stopped by a water rinse followed by 10 min in 0.1 M NaF. The blot was rinsed again in water and dried on filter paper.

Results

Isolation and Enrichment of Thick Filaments

The starting material for this procedure are sections of frozen nematodes prepared according to our previous protocols (4, 5, 19, 21). Instead of disruption of the sections by passage through a French pressure cell, the sections were gently homogenized by hand in a glass apparatus (Dounce). Only ~5% of the potential filaments were liberated, and most of the sections still exhibited muscle birefringence by polarized light microscopy. This observation suggests that the myofibrillar structures within these sections remained organized under these gentle conditions. The thick filaments were more native by the criteria of length and content of myosin and paramyosin (see below) than filaments of previously reported preparations (18, 21). This gentle homogenization and the inclusion of 0.5 M sucrose maintained the integrity of most cell nuclei that were also released, thereby minimizing the release of chromatin, which can bind myosin and filaments. The nuclei, filaments, and other cell structures contained in this homogenate are depicted in the electron micrograph of Fig. 2 *A*, and the proteins of the thick and thin filaments and the histones of the nuclei are prominent in the SDS-PAGE separation of Fig. 3 *A*.

The homogenate was centrifuged at 5,000 *g* for 10 min to sediment the nuclei. Fig. 3 *B* shows the absence of histones in the resulting supernatant. Centrifugation of the supernatant at 15,000 *g* for 30 min provided a pellet enriched in thick filaments but still containing reduced levels of thin filaments, ribosomes, and small nuclei or nuclear fragments. The purification of thick filaments from these contaminants in the 15,000-*g* pellet is shown by comparing Fig. 2 *B* (resuspended pellet diluted 10-fold) to Fig. 2 *A* (undiluted). There are still small nuclei or nuclear fragments and ribosomes in the background. The biochemical enrichment of myosin heavy and light chains and paramyosin with respect to actin is evident (cf. Fig. 3 *C* with Fig. 3 *A* and *B*.

Purification of Thick Filaments

Sedimentation of rabbit psoas muscle filament suspensions in gradients of varying glycerol concentration from 10 to 30% (vol/vol) permitted separation of thick and thin filaments (23). We have adapted this procedure to the separation of structures in the nematode 15,000 *g* pellet. A critical prerequisite of this separation was the resuspension of the 15,000-*g* pellet in a minimal volume to maintain sufficient concentration of proteins for maintenance of polymerized

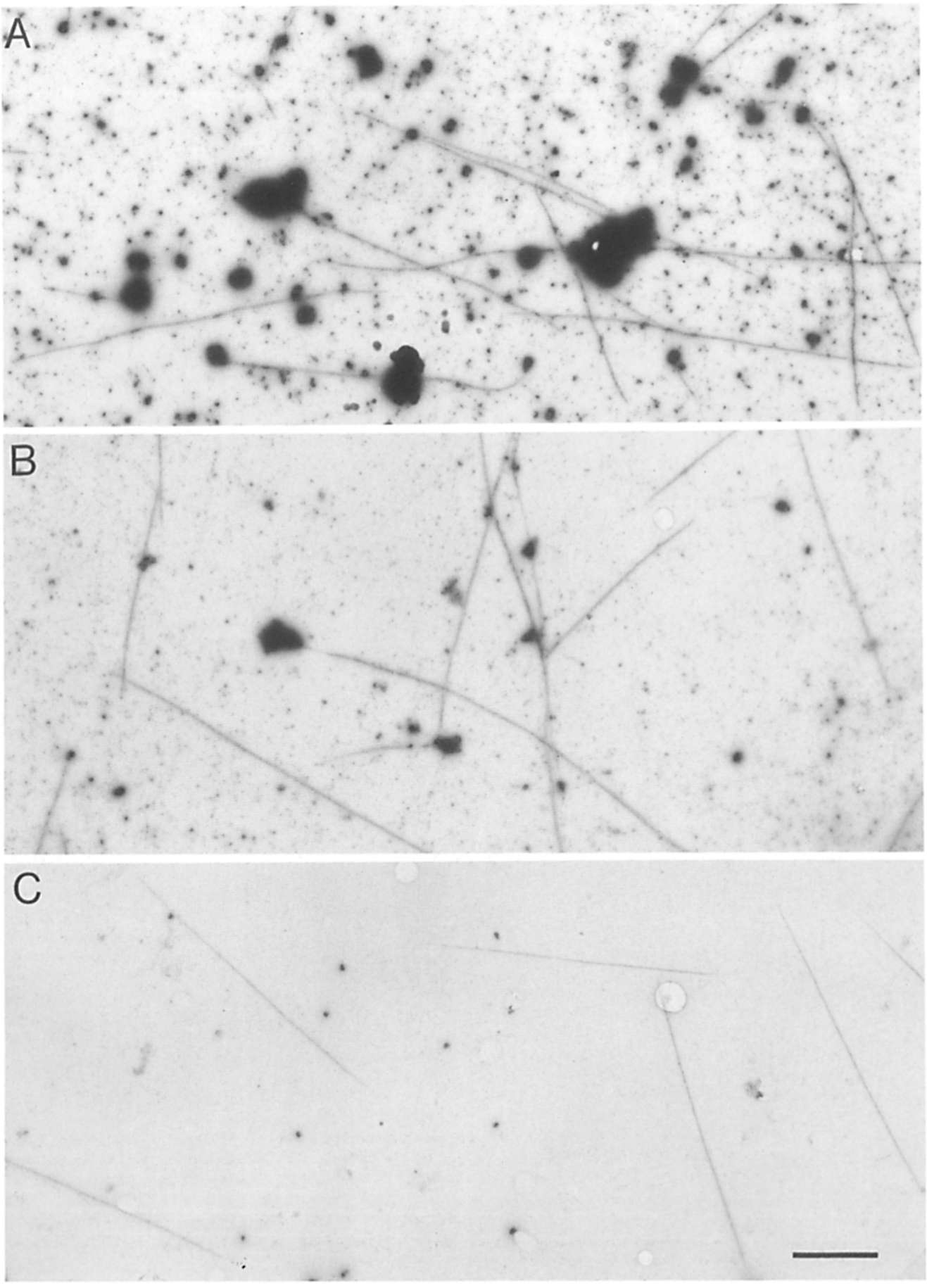
A
B
C

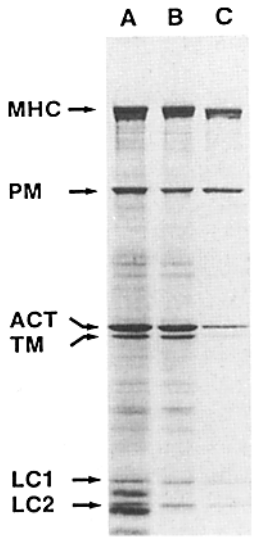

Figure 3. Gel electrophoresis of steps in nematode thick filament purification. (Lane *A*) Second homogenate; (lane *B*) 5,000-*g* supernatant; and (lane *C*) 15,000-*g* pellet. Note loss of low molecular weight histones between lanes *A* and *B* and enrichment of myosin and paramyosin between lanes *B* and *C*. *MHC*, myosin heavy chain; *PM*, paramyosin; *ACT*, actin; *TM*, tropomyosin; *LC1* and *LC2*, light chains 1 and 2 (11). Lanes *A* and *C* of this figure and lanes *A* and *B* of Fig. 2 offer a dual biochemical and morphological comparison.

filaments. After fractionation of the gradient, samples of each fraction were removed for electron microscopy and the remainder of each fraction was centrifuged at 100,000 *g* for 5 h to pellet the contents. The pellets were analyzed by SDS-PAGE to determine their protein composition. Fig. 2 *C* shows, by electron microscopy, a field of a thick filament–enriched fraction comparable with Fig. 2, *A* and *B*. Equivalent areas on grids with equal sample volumes from the fractions most enriched for thick filaments (Fig. 4 *A*), ribosomes (Fig. 4 *B*), and thin filaments and ribosomes (Fig. 4 *C*) are shown at higher magnification. In the peak fractions, such as in Fig. 4 *A*, at least three thick filaments were observed on each grid square with ~2–3 ribosomes per thick filament. One thin filament or its fragment was observed every 9–10 thick filaments in these fractions. Small electron-dense particles, which are likely to be nucleosome-sized chromatin fragments, were also observed.

The purified thick filaments of the peak fractions retained the mean length of the isolated filaments in the original ho-

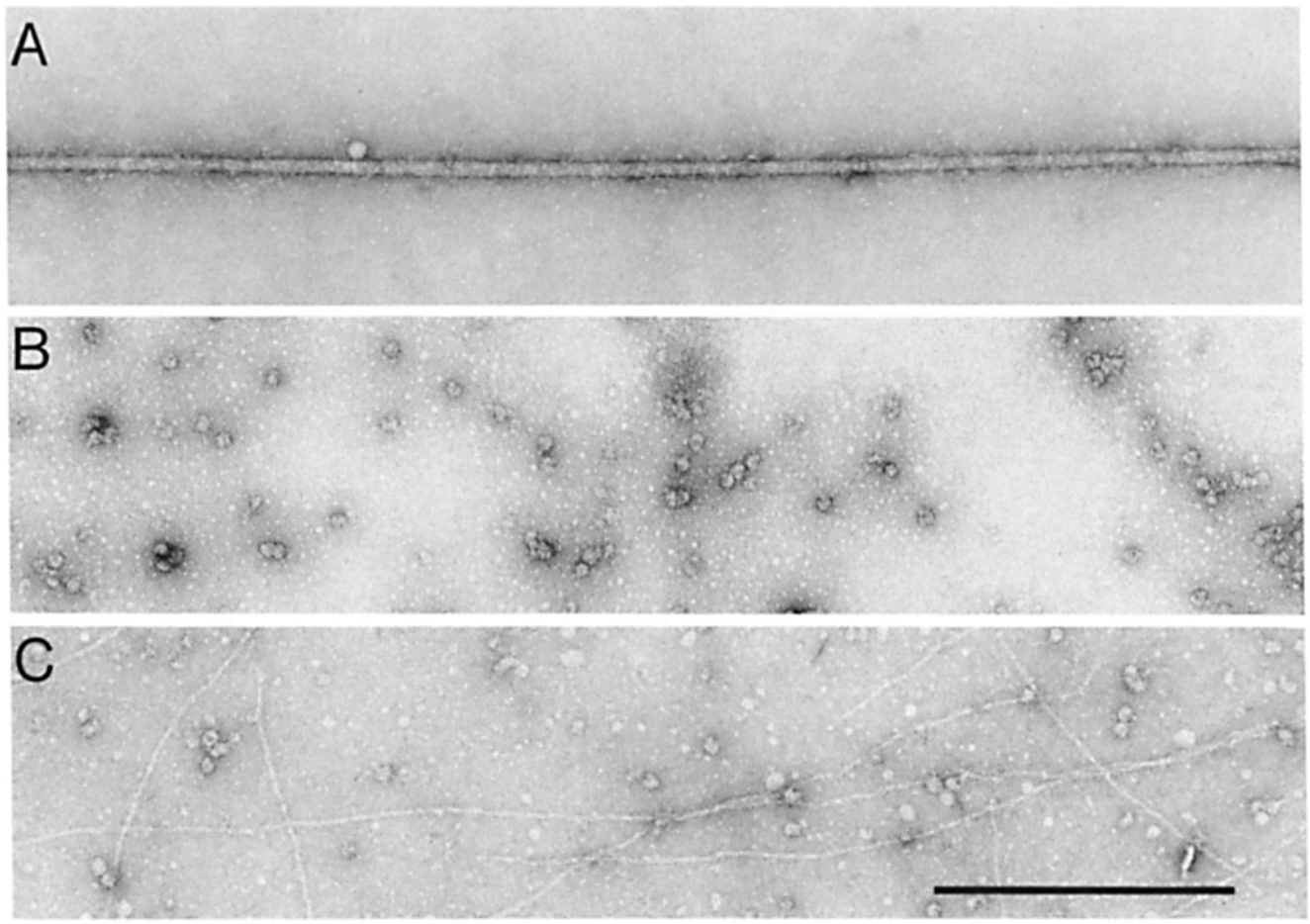

Figure 4. Electron microscopy of different gradient fractions. (*A*) Thick filament–enriched fraction 5; (*B*) ribosome-enriched fraction 9; and (*C*) thin filament–enriched (also ribosomes) fraction 11 of a 10–15% glycerol gradient sedimentation. The micrographs are of equal sample volumes and equal grid areas. Bar, 0.5 μm.

Figure 2. Electron microscopy of steps in nematode thick filament purification. (*A*) Second homogenate; (*B*) 15,000-*g* pellet, resuspended; and (*C*) peak fraction of 10–30% glycerol gradient. Note marked decreases in electron-dense nuclear material, particulate ribosomes, and thin filaments, while thick filament number decreases by about twofold in equivalent samples and areas of observation. Bar, 2 μm.

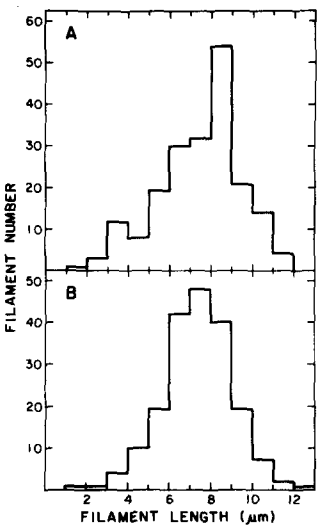

Figure 5. Thick filament length distribution during purification. (*A* and *B*) Thick filaments of second homogenate and enriched fractions of glycerol gradient, respectively. For *A*, mean length = 7.4 μm, SD = 2.0 μm, n = 198. For B, mean length = 7.3 μm, SD = 2.0 μm, n = 195. In both cases, most filaments have been broken at least once, but substantial fractions of thick filaments are ≥9.0 μm, consistent with the native length (16, 33). The difference in mean length does not appear significant, but the distribution of purified filament lengths appears more homogeneous and Gaussian.

mogenate. Fig. 5 compares the histograms of filament number as a function of length of the two populations as determined by electron microscopy. The distributions are similar with the homogenate and gradient thick filaments exhibiting means and SDs of 7.4 ± 2.0 and 7. 3 ± 2.0 μm, respectively. The most frequent filaments are greater than half-native length. Although a small fraction of filaments at each step appear to be of native length, ≥10 μm, another small fraction of filaments shorter than half-native length increases slightly during the preparation.

We observed, for every 10 thick filaments of mean length 7.3 μm, 30 ribosomes and 1 thin filament fragment of approximate length 3.0 μm in the fractions most enriched for thick filaments. By using published estimates for calculating the relative masses of these structures (29, 32) and assuming equal absorption of these structures to the grids, only 1–2% of the mass may be attributed to the contaminating ribosomes and thin filaments. Electron microscopy is a particularly sensitive assay for ribosomes because of their distinct and characteristic morphology. Biochemical detection and quantitation of proteins is less sensitive in the case of ribosomes because of the >1,000-fold difference in the masses of nematode thick filaments and ribosomes and the large number of different proteins constituting the ribosomes.

The protein compositions of 12 gradient fractions and a pellet that formed at the bottom of the gradient were analyzed by SDS-PAGE and Coomassie Brilliant Blue staining (Fig. 6). Fractions 4–7 were reproducibly most enriched for known nematode thick filament proteins: myosin heavy chain (M_r = 229,000), paramyosin (M_r = 108,000), and myosin light chains (M_r = 18,000 and 16,000) (12, 19, 20). Several bands equal to or less than the intensity of the myosin light chains were detected in the 110–200-kD range, and actin was detected as a very faint band. In contrast, fractions 9–11 were most enriched for what are most likely the multiple ribosomal proteins, and fractions 10–12 were most enriched for actin and tropomyosin, the major components of nematode thin filaments (13). The gradient pellet sample was similar in its protein composition to the 15,000-*g* pellet fraction that was placed onto the glycerol gradient. The yields of purified thick filaments varied inversely with the percentage of material in the gradient pellets.

The ratio by densitometry of myosin heavy chain to paramyosin in the thick filament-enriched fraction, 1.6 ± 0.19:1.0 (±SD; n = 8), is similar to the ratio of the bands in nematode homogenates (34). Since myosin heavy chain and paramyosin have similar color values by Coomassie Brilliant Blue staining (9) and nematode myosin heavy and light chains are equivalent stoichiometrically (12), the 16-kD light chain represents 4% by weight of the known thick filament components in the appropriate gradient fractions. The 110–200-kD bands therefore were each <4% of the detected proteins. By Coomassie Brilliant Blue staining of proteins, the thick filaments of the enriched fractions were at least

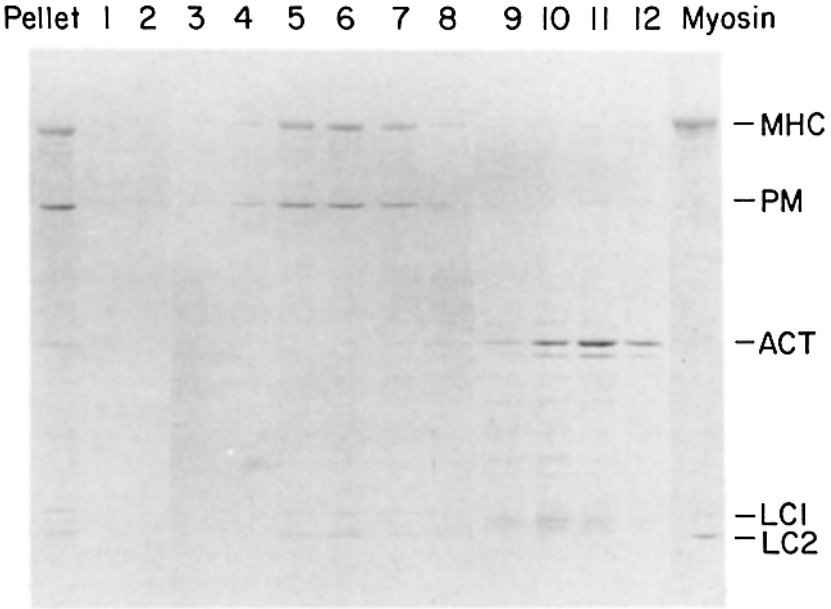

Figure 6. Gel electrophoresis of gradient fractions. Coomassie Blue staining of 7.5–15% SDS-PAGE. Pellet and fractions 1–12 from 10–30% glycerol gradient sedimentation. Column-purified myosin is for comparison (10). Protein designations are the same as in Fig. 3. Fractions 5, 9, and 11 of this figure and Fig. 4, *A–C*, offer biochemical and morphological comparison. The protein bands between myosin heavy chain and paramyosin in the gradient fractions enriched for thick filaments (fractions 5–7) differ in mobility from the bands beneath myosin heavy chain in the purified myosin. The pellet sample shows a mixture of the protein bands present in the fractions.

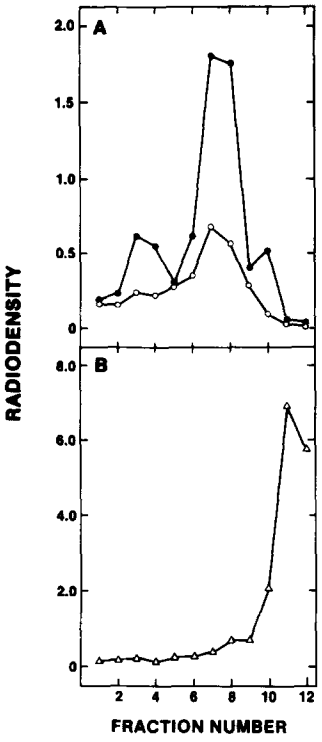

Figure 7. Distribution of myosin, paramyosin, and actin in gradient sedimentations. Densitometry of radioautographs of dried 7.5–15% SDS-PAGE separations of 10–30% glycerol gradient sedimentation fractions of ^{35}S-labeled nematode structures. (*A*) Myosin heavy chain band density (●); paramyosin band density (○). (*B*) Actin band density (△). The absolute scale of radiodensity is the same in *A* and *B*.

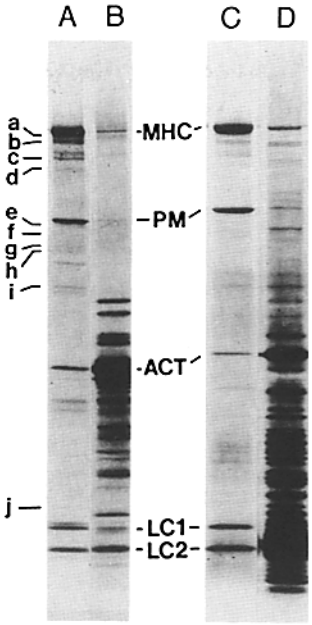

Figure 8. Proteins indexed to thick filaments. Gradient fractions most enriched for (*A* and *C*) thick filaments and (*B* and *D*) thin filaments from radioautogram of (*A* and *B*) ^{35}S-labeled material and (*C* and *D*) silver-stained unlabeled material. Bands *a–j* were consistently found most enriched in thick filament fractions of multiple purifications from wild-type nematodes. *A* and *B* and *C* and *D* are from different 7.5–15% SDS-PAGE.

95% pure. On the other hand, any component or contamination that was present at only 1–2% or less of the total protein would probably not have been detected. Other methods for protein detection were used for the detection of additional proteins at these low levels.

Thick filaments were isolated and purified from ^{35}S-labeled nematodes. SDS-PAGE and radioautography of the gradient fractions was performed. Densitometry of the radioautographic bands of myosin heavy chain, paramyosin, and actin offered a graphical representation of the separation of these proteins in the 12 fractions (Fig. 7). The myosin and paramyosin bands clearly peaked together in fractions 7 and 8, whereas actin peaked in fraction 11. This analysis permits indexing of minor bands to one structure or the other by coenrichment with the known major components.

Analysis of Associated Proteins of Thick Filaments

Silver staining of SDS-PAGE of unlabeled preparations and radioautography of preparations from nematodes endogenously labeled with ^{35}S were conducted to detect minor proteins associated with thick filaments. These methods of detection are more sensitive than Coomassie Brilliant Blue staining, although they are not as useful for quantitative comparisons between kinds of proteins. We found significant variation in the relative silver staining and ^{35}S labeling of different proteins compared to their relative Coomassie Brilliant Blue intensities. Differences in the reactions of the two stains, contents of sulfur-containing amino acids, and turnover of specific proteins in addition to differences in concentrations of the proteins all contribute to the relative intensities of the proteins. Minor proteins cosedimenting with the known thick filament proteins and structures in the gradient were indexed as thick filament–associated proteins. Proteins that were most enriched in the ribosome and thin filament fractions were considered to be contaminants of the thick filament fractions.

Inspection of all the fractions revealed minor bands that cosedimented with thick filaments and others that cosedimented with either ribosomes, thin filaments, or with none of the recognizable structures. Minor bands detected by both silver staining and ^{35}S labeling were indexed to thick filaments on the basis of cosedimentation and the demonstrated purity of the thick filaments. Fig. 8, *C* and *D*, shows SDS-PAGE separations of fractions 5 and 10 in Fig. 5 after silver staining. 10 minor bands appeared to enrich with myosin and paramyosin in fractions 4–8, whereas other bands in these fractions were likely to be contaminants from ribosomes and thin filaments since they were most enriched in fractions 9–12. Fig. 8, *A* and *B*, shows radioautograms of the SDS-PAGE of fractions 7 and 11 from the ^{35}S-labeled preparation. Bands at the same positions of the indexed bands in Fig. 8 *A* were also detected in Fig. 8 *C*. The minor bands of the ribosome and thin filament–containing fractions of the radioautogram (Fig. 8 *B*) showed a similar but distinct pattern from the silver staining in Fig. 8 *C*. This difference is more likely due to differences in staining and labeling of the specific proteins. The concordance of the experiments using silver staining and ^{35}S labeling in detecting the same indexed bands offers strong support for these entities being proteins associated with thick filaments. Bands b, c, d, f, g, and h also stained with Coomassie Blue (see Figs. 6 and 12).

Fig. 9 is a plot of the relative mobilities of these thick filament–associated proteins and their relative molecular masses derived from the mobilities and known relative molecular masses of myosin heavy and light chains, paramyosin, actin, and commercially available protein markers. All of these proteins were of lower relative molecular mass than

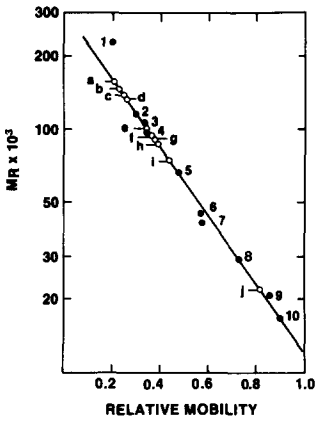

Figure 9. Mobilities of thick filament-indexed proteins. *a–j* (○) correspond to the bands shown in Fig. 7. Standards (●) and their relative molecular masses are (*1*) nematode myosin heavy chain (229,000), (*2*) bacterial β-galactosidase (116,000), (*3*) nematode paramyosin (108,000), (*4*) rabbit muscle glycogen phosphorylase b (97,800), (*5*) BSA (66,000), (*6*) nematode actin (42,000), (*7*) nematode tropomyosin (38,000), (*8*) bovine erythrocyte carbonic anhydrase (29,000), (*9*) nematode light chain 1 (18,000), and (*10*) nematode light chain 2 (16,000).

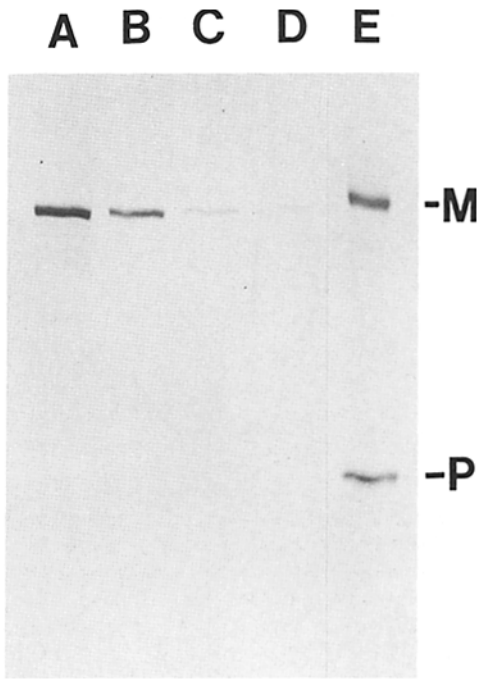

Figure 10. Antimyosin and antiparamyosin reaction with purified thick filaments. Reaction of nitrocellulose blot of 5% SDS-PAGE with combination of mAbs specifically reactive with myosin A (5–6), myosin B (28.2), and paramyosin (5–23). (*A–D*) 1.5, 0.75, 0.38, and 0.19 μg of purified myosin as standards. (*E*) Pooled fractions 4–7 of 10–30% glycerol gradient sedimentation. Note that antibodies can detect 12.5% or less of most intense bands and several minor bands beneath the heavy chain of purified myosin in *A*. No minor bands react in gradient fraction sample.

myosin heavy chain. Four were intermediate in mobility between myosin heavy chain and paramyosin; the rest were lower in relative molecular mass than paramyosin. It should be noted that several of these bands (a–d particularly) appeared to be doublet or triplet in character but the sub-bands were so close together so as to prevent individual measurement. More detailed analysis of such bands is necessary for further clarification of the status of the fine individual sub-bands. Two bands at ~250 and 300 kD are seen in many but not all preparations (see Fig. 12). Because of this inconstancy, these bands were not indexed.

The observation that all of the indexed minor proteins detected were of lower relative molecular mass than myosin heavy chain and most were lower in relative molecular mass than paramyosin raised the question as to whether these additional bands were degradation products of either myosin or paramyosin. To minimize such possibilities, a battery of protease inhibitors was included throughout the preparation of the thick filaments. Without such precautions, myosin and paramyosin become degraded.

To test for proteolysis of myosin and paramyosin more directly, samples of previously purified, stored myosin and paramyosin and of fresh, pooled gradient fractions 4–7 were subjected to electrophoresis in separate lanes. A nitrocellulose replica was prepared (31) and reacted with mAbs 5-6, 28.2, and 5-23 specific to the major myosin heavy chains A and B and paramyosin components, respectively (Fig. 10). The purified protein showed multiple very faint bands at relative molecular masses lower than the major myosin heavy chain band (Fig. 10 *A*). Previous work has shown that these bands are degradation products of myosin heavy chain B (21). These bands stain at ~10% of the intensity of the intact myosin heavy chain as shown by the dilution series. In contrast, equivalent amounts of myosin heavy chain and paramyosin in the thick filament preparation did not produce reactive bands at other relative molecular masses (Fig. 10 *E*). Comparison of the lower relative molecular mass bands in the preparations of purified myosin with the 10 indexed bands of the thick filaments indicated that their mobilities on SDS-PAGE were not identical.

Evidence for the Association of the Indexed Proteins with Core Structures

Previous reports have described the isolation of thick filaments from the myosin B–deficient mutant CB190 and the paramyosin-deficient mutant CB1214 (4, 18, 21). The thick filament proteins from these strains serve here as controls for the indexed protein bands not being derived from either myosin B or paramyosin. Since both these filament preparations exhibit hollow-appearing core-type structures, they should contain specific structural proteins of the cores. The CB1214 mutant filaments have a net loss of mass due to the absence of paramyosin and reduced myosin B binding in the polar regions (5, 18), which correlates with their slightly lower sedimentation velocity in 10–30% glycerol gradients (Fig. 11). Electrophoretograms of the peak thick filament fractions of this abnormally migrating mutant species as well as the peak fractions of normally migrating CB190 consistently showed 6 of the 10 indexed wild-type protein bands on SDS-PAGE (Fig. 12, *B* and *C*). These bands have the same mobilities as bands b, c, d, f, g, and h of native wild-type filaments. Their presence in the slowly migrating CB1214 thick filaments suggests that these protein bands are not part of some particle or particles that adventitiously comigrate with wild-type thick filaments. Bands a and e of wild-type thick filaments are absent in the myosin B–deficient and paramyosin-deficient mutant filaments, respectively. These proteins are

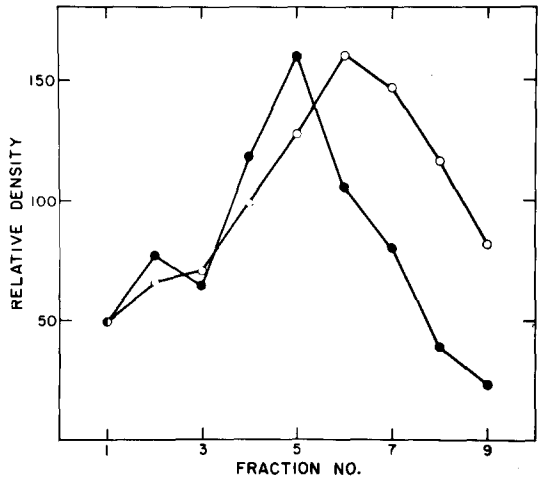

Figure 11. Sedimentation of wild-type and paramyosin-deficient mutant thick filaments. The myosin heavy chain bands of silver-stained SDS-PAGE of 10–30% glycerol gradient sedimentation of wild-type N2 (●) and paramyosin-deficient mutant CB1214 (○) were densitometered. The results of two analyses per stain were averaged and the peaks of maximum density were normalized with respect to one another.

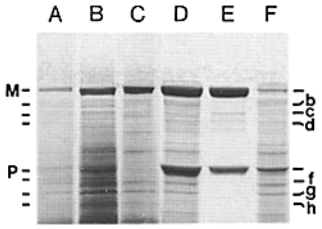

Figure 12. Identification of indexed bands in native mutant and chemically dissociated wild-type thick filaments. (*A*) Gradient-purified wild-type thick filaments dissociated by KSCN and resedimented; (*B*) CB190 myosin B-deficient gradient purified thick filaments; (*C*) CB1214 paramyosin-deficient gradient purified thick filaments; (*D*) gradient pellets of wild-type preparation treated with KSCN before resedimentation; (*E*) supernatant of resedimentation of *D*; and (*F*) pellet of resedimentation of *D*. *A–C* are silver stained and *D–F* are Coomassie Blue stained 7.5–15% SDS-PAGE. *M*, myosin heavy chain; *P*, paramyosin. *b–d* and *f–h* are the same designations as in Figs. 8 and 9. These six indexed bands are preserved in *A–D* and *F* but are not detected in *E*.

either products of the missing major components or may be proteins which require the presence of the missing component for their more peripheral association with thick filaments.

Fig. 12 *A* shows SDS-PAGE of gradient purified wild-type thick filaments that were treated with 50 mM KSCN, pH 8.0, and pelleted after partial dissociation. The myosin and paramyosin have been partially solubilized. All of the additional protein bands present in the mutant filaments that were indexed to native wild-type thick filaments were observed in this preparation. The thick filaments of the 15,000-*g* pellet or the gradient pellet can be more completely dissociated than the more purified filaments and still show at least six indexed protein bands. In both of these fractions, chromatin and actin filaments are present at significant levels. Possibly, interaction of solubilized myosin and paramyosin with these structures promotes their dissociation from thick filaments. In the present procedure, no proteolysis of soluble paramyosin occurred unlike the situation in the cruder preparations of previous reports (4, 5). Fig. 12, *D–F*, shows a gradient pellet and the 25,000 *g* supernatant and pellet derived from it by treatment with 50 mM KSCN, pH 8.2. About 90% of the myosin heavy chain and 75% of the paramyosin, as determined by densitometry, were solubilized, but the six indexed bands, b, c, d, f, g, and h, remained with the pelleted core structures. Several of these bands are doublets or triplets like in native thick filaments. A set of nonthick filament–indexed bands of mobilities similar to myosin heavy chain fragments (Fig. 10 *A*) but distinct from the indexed, pelleted bands were solubilized in addition to the myosin and paramyosin.

Fig. 13 *A* shows the typical appearance of CB1214 thick filaments including their hollow-appearing flanking polar regions that may be compared to native wild-type thick filaments of Fig. 4 *A*. Fig. 13, *B–D*, shows central and flanking core structures, polar core structures, and additional short structures produced from KSCN-treated wild-type thick filaments (compare with native wild-type thick filaments in Fig. 4 *A*). The structures seen in Fig. 13 *D* have not been described previously. They have diameters of ~9 nm and lengths between 100 and 200 nm. They may represent short fragments of terminal polar core structures which taper to diameters <10 nm or of the central core material previously postulated to be within the central regions of the filaments that are 30 nm or greater in diameter (4). The flanking core structures of Fig. 13 *B* are ~18 nm in diameter, in contrast to the 13–14-nm diameter of the CB1214 mutant or of wild-type

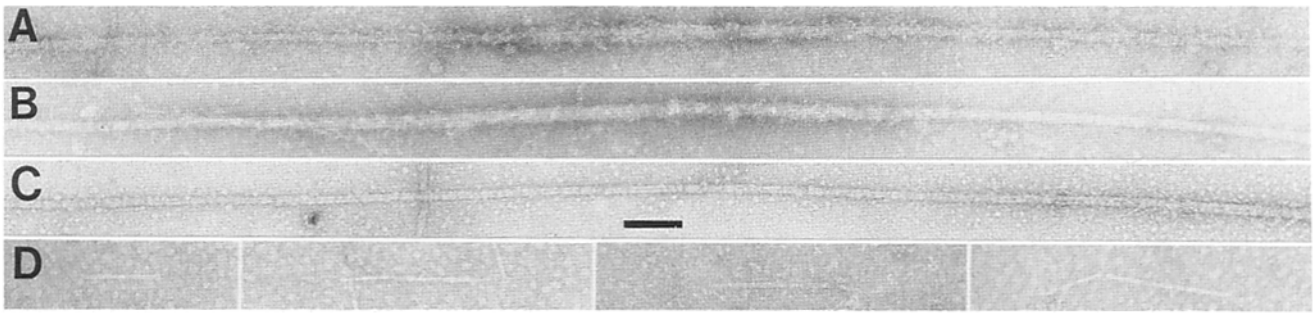

Figure 13. Electron microscopy of CB1214 and dissociated wild-type structures. (*A*) CB1214 thick filament, central region, and flanking polar structures; (*B–D*) wild-type KSCN dissociated structures ([*B*] central region and flanking core structures, [*C*] polar core structure, and [*D*] multiple short structures). Bar, 100 nm.

polar core structures (Fig. 13, *A* and *C*). This increased diameter in dissociated wild-type filaments may reflect remaining paramyosin consistent with the gel analysis of Fig. 12 *F*. The central regions of CB1214 and dissociated wild-type filaments in Fig. 13, *A* and *B*, are ~30 nm in diameter and have been shown previously to have myosin at their surfaces (4, 5), consistent with the remaining myosin in the gel analyses of Fig. 12, *A*, *C*, and *E*.

Thus, six indexed protein bands which cosedimented with wild-type and mutant thick filaments were detected in the genetic absence of myosin B or paramyosin (the two most significant protein components) and remained with the dissociated filament structures after KSCN treatment. These results suggest that the six bands are likely not only to be additional components of the thick filaments but candidates for the putative core structure components. There appeared to be additional protein bands at relative molecular masses greater than that of myosin heavy chain in Fig. 12, *B–F*, but not in Fig. 12 *A* or Fig. 7, *A* and *C*. These protein bands may reflect core structure components as well, but their inconstant appearance requires further experimental work for their identification.

Discussion

Thick filaments have been purified that retain greater than one-half of the full length in situ, averaging 7.3 μm (18, 35). Further evidence for retention of native properties is maintenance of the weight ratio of myosin heavy chain to paramyosin of 1.6:1.0 of homogenates (35) in the purified thick filament preparations. The final purification step, glycerol gradient sedimentation, separates the thick filaments from most contaminating ribosomes and thin filaments and yields >95% pure structures on the basis of both protein analysis and morphological examination. This purity is comparable to that achieved with rabbit psoas muscle thick filaments (23). The procedure reported here is likely to be applicable to the isolation of thick filaments from other organisms of practical interest such as parasitic nematodes and schistosomes (17, 26).

Yields and enrichments were not determined quantitatively for the overall purification or for most steps. The theoretical maximum for enrichment of thick filaments from whole nematodes on the basis of myosin and paramyosin content can be only 50-fold (11). This enrichment was approached in the glycerol gradients sedimentation on the basis of purity. The yields of purified thick filaments from whole nematodes are very small (<1%) but comparable to the rabbit striated muscle preparations (7, 23). The greatest losses occur at homogenization (95% remain in the sections), the 15,000-*g* sedimentation (50% remain in the supernatant with most of the ribosomes and thin filaments), and the glycerol gradients sedimentation (variably 50–75% pellet in association with chromatin). The purified thick filaments nevertheless reflect the properties of native body-wall thick filaments in terms of length, distribution of myosins A and B (data not shown), and myosin/paramyosin ratios that were observed in either intact nematodes or crude preparations (18, 21, 35).

At least 10 minor protein bands, a–j (each of which may represent more than one polypeptide), cosediment with the thick filaments in that they are most enriched in gradient fractions having the highest concentrations of myosin heavy chain and paramyosin (biochemically) and thick filaments (morphologically). These proteins do not appear to be degradation products of either myosin or paramyosin. However, one or more bands may be derived from possible nematode analogues of muscle nebulin and titin (33, 34) or from the large putative *unc-22*-encoded polypeptide (22), which have native relative molecular masses >400,000 and are easily degraded. Six of the cosedimenting bands–b, c, d, f, g, and h–are present in dissociated wild-type thick filaments and in thick filaments prepared from myosin B–deficient and paramyosin-deficient mutants. The mutant results demonstrate that these minor proteins cannot be derived from either myosin B or paramyosin, the major thick filament components in which degradation has been observed in previous preparations (12, 18, 21, 35). Myosin A shows little or no degradation (21). The paramyosin-deficient mutant filaments sediment differently than wild-type thick filaments, further indicating specific association between the six proteins and thick filaments. The paramyosin-deficient mutant thick filaments and the dissociated wild-type structures resemble each other morphologically. These results suggest that the six associated proteins may be candidates for the putative components of the central and polar core structures proposed previously (4).

A schematic diagram of a model that indicates the relative positions of thick filament proteins is shown in Fig. 14. Our present experiments cannot distinguish between this model and a closely related model in which some of the additional components may complex with paramyosin to form the polar core structures in wild-type thick filaments. That the core structures in central regions may not contain paramyosin is suggested by the similarity in diameter and internal density of the central regions of wild-type and CB1214 paramyosin-deficient filaments (Fig. 13, *A* and *B*) (4, 18). The most central regions of A bands in several invertebrate muscles (3) in-

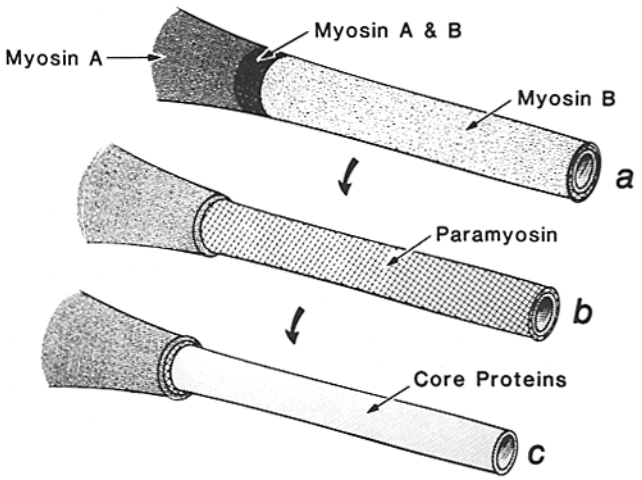

Figure 14. Model of localization of thick filament proteins. Schematic diagrams of portions of filaments with central regions containing myosin A at left and polar regions at right. (*a*) Myosin-covered native thick filament; (*b*) paramyosin-covered partially dissociated thick filament; and (*c*) more extensively dissociated thick filament. *Core Proteins* refers to internal proteins of both polar and central regions, which may not be identical. Core proteins may interact with paramyosin or one of the myosin isoforms in more complex arrangements than shown here. (Modified figure from reference 4.)

cluding the body-wall muscles of *C. elegans* (Hoskins, R., and H. F. Epstein, unpublished results) exhibit an absence of antiparamyosin labeling in light microscopic experiments. The short 9-nm structures observed in KSCN-dissociated preparations (Fig. 13 *D*) may be related to the core structure of the central regions.

The availability of purified thick filaments and their dissociation into core structures will provide appropriate material for the production and characterization of antibodies to the minor proteins. These immunological reagents will be necessary for the identification by immunochemical localization at the ultrastructural level of these proteins as components of the core structures and for the determination of their structural relationship to paramyosin. Studies of the reconstitution of thick filaments from purified components from wild-type and mutant nematodes can now be undertaken to test whether during assembly the core structures are necessary for the specific localization of myosins A and B (4, 5, 21) and the precise determination of native length (18).

The results obtained with *C. elegans* are likely to be of specific relevance to the problem of thick filament structure and assembly in other species. In addition to the thick filaments from other nematodes (26), the filaments of certain insect indirect flight muscles are likely to require additional components associated with core structures. The thick filaments of *Musca domestica* (housefly) and *Sarcophaga bullata* (blowfly) contain only 2% paramyosin (*Musca*), have lengths of ~2.8 μm in contrast to the 1.5-μm-long "myosin" filaments of vertebrates (23), and exhibit prominent hollow-appearing cores (24, 25). In preliminary experiments, we have identified protein bands in thick filaments purified from the blowfly that upon electrophoresis migrate similarly to bands b, c, d, f, g, and h of the nematode. The similarity of *Drosophila* thick filaments to these other *Dipteran* structures (10) suggests that genetic dissection of the core structure and its relation to assembly may be feasible in this organism as well as in *C. elegans*.

We are indebted to Dr. Stanley H. Appel for his continuing interest and support of this research. We thank Steven Alexander for his contributions during two summers to this work; Drs. Sandra Honda and M. R. Sivaramakrishnan for their invaluable advice on various methods; and Drs. Kimon J. Angelides and Warren J. Strittmatter for suggestions on the manuscript.

The research was supported in part by grants from the Jerry Lewis Neuromuscular Dystrophy Association, the Welch Foundation, and the National Institute of General Medical Sciences. The Word Processing Center provided outstanding service in the preparation of this manuscript.

Received for publication 4 December 1987, and in revised form 5 February 1988.

References

1. Bennett, P., R. Craig, R. Starr, and G. Offer. 1986. The ultrastructural localization of C-protein, X-protein, and H-protein in rabbit muscle. *J. Muscle Res. Cell Motil.* 7:550–567.
2. Brenner, S. 1974. The genetics of *Caenorhabditis elegans*. *Genetics.* 77:71–94.
3. Elfvin, M., R. J. C. Levine, and M. M. Dewey. 1976. Paramyosin in invertebrate muscles. I. Identification and localization. *J. Cell Biol.* 71:261–272.
4. Epstein, H. F., D. M. Miller III, I. Ortiz, and G. C. Berliner. 1985. Myosin and paramyosin are organized about a newly identified core structure. *J. Cell Biol.* 100:904–915.
5. Epstein, H. F., I. Ortiz, and L. A. Traeger Mackinnon. 1986. The alteration of myosin isoform compartmentation in specific mutants of *Caenorhabditis elegans*. *J. Cell Biol.* 103:985–993.
6. Epstein, H. F., R. H. Waterston, and S. Brenner. 1974. A mutant affecting the heavy chain of myosin in *Caenorhabditis elegans*. *J. Mol. Biol.* 90:291–300.
7. Etlinger, J. D., R. Zak, and D. A. Fischman. 1976. Compositional studies of myofibrils from rabbit striated muscle. *J. Cell Biol.* 68:123–141.
8. Garcea, R. L., F. Schachat, and H. F. Epstein. 1970.Coordinate synthesis of two myosins in wild-type and mutant nematode muscle during larval development. *Cell.* 15:421–428.
9. Gaylinn, B., and M. M. Dewey. 1986. Paramyosin and myosin content of the thick filament in the striated muscle of *Limulus*. *J. Muscle Res. Cell Motil.* 7:467–473.
10. Goode, M. D. 1972. Ultrastructure and contractile properties of isolated myofibrils and myofilaments from *Drosophila* flight muscle. *Trans. Am. Microsc. Soc.* 91:182–194.
11. Hanson, J., and H. E. Huxley. 1953. Structural basis of the cross-striations in muscle. *Nature (Lond.).* 172:530–532.
12. Harris, H. E., and H. F. Epstein. 1977. Myosin and paramyosin of *Caenorhabditis elegans*: biochemical and strucural properties of wild-type and mutant proteins. *Cell.* 10:709–719.
13. Harris, H. E., M-Y. W. Tso, and H. F. Epstein. 1977. Actin and myosin-linked calcium regulation in the nematode *Caenorhabditis elegans*. Biochemical and structural properties of native filaments and purified proteins. *Biochemistry.* 16:859–865.
14. Huxley, H. E. 1963. Electron microscope studies on the structure of natural and synthetic protein filaments from striated muscle. *J. Mol. Biol.* 7:281–308.
15. Huxley, H. E., and J. Hanson. 1954. Changes in the cross-striations of muscle during contraction and stretch and their structural interpretation. *Nature (Lond.).* 173:973–976.
16. Josephs, R., and W. F. Harrington. 1966. Studies on the formation and physical chemcial properties of synthetic myosin filaments. *Biochemistry.* 5:3474–3487.
17. Lanar, D. E., E. J. Pearce, S. L. James, and A. Sher. 1986. Identification of paramyosin as schistosome antigen recognized by intradermally vaccinated mice. *Science (Wash. DC).* 234:593–596.
18. Mackenzie, J. M., Jr., and H. F. Epstein. 1980. Paramyosin is necessary for determination of nematode thick filament length *in vivo*. *Cell.* 22: 747–755.
19. Mackenzie, J. M., Jr., and H. F. Epstein. 1981. Electron microscopy of nematode thick filaments. *J. Ultrastruct. Res.* 76:277–285.
20. McLachlan, A. D., and J. Karn. 1983. Periodic features in the amino acid sequence of nematode myosin rod. *J. Mol. Biol.* 164:605–626.
21. Miller, D. M., III, I. Ortiz, G. C. Berliner, and H. F. Epstein. 1983. Differential localization of two myosins within nematode thick filaments. *Cell.* 34:477–490.
22. Moerman, D. G., G. M. Benian, and R. H. Waterston. 1986. Molecular cloning of the muscle gene *unc-22* in *Caenorhabditis elegans* by Tc1 transposon tagging. *Proc. Natl. Acad. Sci. USA.* 83:2579–2583.
23. Morimoto, K., and W. F. Harrington. 1973. Isolation and composition of thick filaments from rabbit skeletal muscle. *J. Mol. Biol.* 77:165–175.
24. Reedy, M. K., G. F. Bahr, and D. A. Fischman. 1972. How many myosins per cross-bridge? I. Flight muscle myofibrils from the blowfly, *Sarcophaga bullata*. *Cold Spring Harbor Symp. Quant. Biol.* 37:397–421.
25. Reedy, M. K., K. R. Leonard, R. Freeman, and T. Arad. 1981. Thick myofilament mass determination by electron scattering measurements with the scanning transmission electron microscope. *J. Muscle. Res. Cell Motil.* 2:45–64.
26. Rosenbluth, J. 1965. Ultrastructural organization of obliquely striated muscle fibers in *Ascaris lumbricoides*. *J. Cell Biol.* 25:495–515.
27. Schachat, F., R. L. Garcea, and H. F. Epstein. 1978. Myosins exist as homodimers of heavy chains: demonstration with specific antibody purified by nematode mutant myosin affinity chromatography. *Cell.* 15: 405–411.
28. Schachat, F. H., H. E. Harris, and H. F. Epstein. 1977. Two homogeneous myosins in body-wall muscle of *Caenorhabditis elegans*. *Cell.* 10:721–728.
29. Squire, J. M. 1971. General model for the structure of all myosin-containing thick filaments. *Nature (Lond.).* 233:457–462.
30. Szent-Györgyi, A. G., C. Cohen, and J. Kendrick-Jones. 1971. Paramyosin and the filaments of molluscan "catch" muscles. II. Native filaments: isolation and characterization. *J. Mol. Biol.* 56:239–258.
31. Towbin, H., T. Staehelin, and J. Gordon. 1979. Electrophoretic transfer of proteins from polyacrylamide gels to nitrocellulose sheets: procedure and some applications. *Proc. Natl. Acad. Sci. USA.* 76:4350–4354.
32. Van Holde, R. E. 1971. Physical Biochemistry. Prentice-Hall Inc., Englewood Cliffs, NJ. 246 pp.
33. Wang, K., J. McClure, and A. Tu. 1979. Titin: major myofibrillar components of striated muscle. *Proc. Natl. Acad. Sci. USA.* 76:3698–3702.
34. Wang, K., and C. L. Williamson. 1980. Identification of an N2 line protein of striated muscle. *Proc. Natl. Acad. Sci. USA.* 77:3254–3258.
35. Waterston, R. H., H. F. Epstein, and S. Brenner. 1974. Paramyosin of *Caenorhabditis elegans*. *J. Mol. Biol.* 90:285–290.
36. Waterston, R. H., R. M. Fishpool, and S. Brenner. 1977. Mutants affecting paramyosin in *Caenorhabditis elegans*. *J. Mol. Biol.* 117:828–842.